# Radiation Damage Accumulation in $\alpha$-$Ga_2O_3$ under P and $PF_4$ Ion Bombardment

© P.A. Karaseov[1], K.V. Karabeshkin[1], A.I. Struchkov[1], A.I. Pechnikov[2,3], V.I. Nikolaev[2,3], V.D. Andreeva[1], A.I. Titov[1]

[1] Peter the Great Saint-Petersburg Polytechnic University,
195251 St. Petersburg, Russia
[2] Ioffe Institute,
194021 St. Petersburg, Russia
[3] Perfect Crystals LLC,
194021 St. Petersburg, Russia

E-mail: Platon.Karaseov@spbstu.ru; Andrei.Titov@rphf.spbstu.ru

*Received July 3, 2022*
*Revised July 31, 2022*
*Accepted August 4, 2022*

We study radiation damage accumulation in alpha polymorph of gallium oxide ($\alpha$-$Ga_2O_3$) epitaxial layers under irradiation with 40 keV monatomic P and 140 keV molecular $PF_4$ ions. The distribution of stable structural damage is bimodal in both cases. The growth rate of the surface disordered layer under $PF_4$ ion irradiation is significantly higher than that under monatomic P ion bombardment. At the same time, monatomic ion irradiation is more efficient in the bulk defect peak formation. Thus, the density of displacement cascades strongly affects the formation of stable damage in $\alpha$-gallium oxide. The doses required to create the same level of disorder in the metastable $\alpha$-polymorph are higher than that in the thermodynamically stable $\alpha$-. Mechanisms of damage formation in these polymorphs are different.

**Keywords:** gallium oxide, $\alpha$-$Ga_2O_3$, ion bombardment, collision cascades, radiation damage, collision cascade density, defect engineering, radiation resistance.

DOI: 10.21883/SC.2022.09.54132.9928

## 1. Introduction

Semiconductors needed to construct high-power electronic next-generation optoelectronic devices have been extensively searched for and examined in recent years [1]. Gallium oxide $Ga_2O_3$ is one of the most promising materials in this context, since it offers such advantages as a wide band gap (4.5−5.3 eV for different phases) and high values of the breakdown voltage ($\sim$ 8 MV/cm), electron mobility, and thermal conductivity [2–4]. It may form various crystal phases ($\alpha$-, $\beta$-, etc. [2]. The majority of studies of gallium oxide published to date are focused on the properties of $\beta$-$Ga_2O_3$, which is thermodynamically stable under atmospheric temperature and allows one to grow perfect bulk crystals using, e.g., the edge-defined film-fed growth (EFG) method or zone melting [2,3,5]. At the same time, $\alpha$-$Ga_2O_3$ has a wider band gap than the $\beta$-phase (5.3 eV as compared to 4.85 eV) [3]. Therefore, $\alpha$-$Ga_2O_3$ may feature an even higher breakdown voltage. In addition, $\alpha$-$Ga_2O_3$ has a corundum-type crystal structure, which may simplify the fabrication of heterostructures with such materials as AlN [6]. Although the $\alpha$-phase is metastable under atmospheric pressure, the temperature of its transition to the stable $\beta$-phase exceeds 550°C. This may provide an opportunity to construct power electronics devices based on $\alpha$-$Ga_2O_3$ [3,6]. At the same time, the production of $\alpha$-$Ga_2O_3$ of a sound quality has been organized only a short time ago [6,7]. Therefore, its properties still remain understudied.

Ion implantation is one of the key methods used for selective adjustment of properties in the fabrication of semiconductor devices (specifically, for introduction of doping impurities, formation of insulating regions, etc.). Irradiation with accelerated ions inevitably leads to the accumulation of radiation damage in the target. The nature and degree of radiation damage depend in a complex way on a number parameters, such as the mass and energy of an ion, the ion current density, the target temperature, etc. [8]. Ions decelerating in the target collide with lattice atoms, this knocking them out of regular positions, and produce so-called collision cascades of vacancies and interstitial atoms. It was demonstrated experimentally that the density of collision cascades exerts a considerable influence on the resulting radiation damage in Si [9–11], SiC [12], ZnO [13], GaN [14,15], metals [16], polymers [17], etc. Specifically, the defect formation was found to be enhanced in $\beta$-$Ga_2O_3$ [18]. it is also known that a convenient way to study the effects associated with the density of cascades is by comparing the accumulation of damage under irradiation with atomic or molecular ions [9,12–14,17,19]. In our earlier research, we have compiled one of the first sets of data on the accumulation of structural damage in $\alpha$-$Ga_2O_3$ subjected to irradiation with accelerated atomic ions [20]. The aim of the present study is to reveal the influence of the density of collision cascades on the efficiency of

defect formation in epitaxial $\alpha$-$Ga_2O_3$ layers subjected to irradiation with atomic P ions and molecular $PF_4$ ions.

## 2. Experimental procedure

Epitaxial $\alpha$-$Ga_2O_3$ layers with a corundum structure, a thickness of $\sim 2\,\mu$m, and orientation (0001) grown at OOO „Sovershennye Krtistally“ by hydride vapor phase epitaxy (HVPE) on the $c$-plane of a sapphire substrate [21] were examined. Gallium chloride needed for the gas-transport reaction was synthesized directly in the source region of the reactor by flowing gaseous hydrogen chloride (HCl 99.999%) above metallic gallium (Ga 99.9999%). High-purity oxygen (99.998%) required for the production of gallium oxide was fed into the reaction zone. Gallium oxide layers were grown at substrate temperature $T \sim 500^\circ$C under excess oxygen flow. The ratio of VI/III elements fell within the range from 2 to 10. High-purity argon (99.998%) served as the carrier gas. The overall gas flow through the reactor was 10 L/min. The deposition rate varied with the flow of HCl through the gallium source and fell within the range from 2 to 5 $\mu$m/h; the deposition time was chosen so as to obtain the needed film thickness. With the growth completed, the substrate was cooled to room temperature in a flow of argon.

The crystal structure of samples was examined by X-ray diffraction (XRD) at a D8 Advance Bruker Θ-Θ diffractometer with Bragg–Brentano focusing, $U = 40$ kV, and $I = 40$ mA. The diffraction pattern was recorded with a high-speed LynxEye (Bruker) PSD detector with a capture window of 3.2° in 2Θ. The measurement was performed at a pitch of 0.02° with accumulation for 0.7 s at each step. The $K_\alpha$ line of copper was used; panoramic spectra in the range of 15−120° and detailed spectra in the region of $\alpha$-$Ga_2O_3$ reflections were recorded. in addition, the degree of disorder was measured by Rutherford backscattering spectrometry with channeling (RBS/C) in the [0001] direction. $He^{++}$ ions with an energy of 0.7 MeV scattered by 103° with respect to the direction of the incident beam were used in these measurements.

The samples were irradiated with $P^+$ and $PF_4^+$ ions at room temperature in a 500 kV implanter produced by HVEE. Irradiation was performed at an angle of 7° with direction [0001] to minimize the channeling effects. The irradiation parameters were chosen so as to preserve an opportunity for meaningful comparison between the results of irradiation with P and $PF_4$ ions. As was noted earlier [22,23], the following parameters should be kept unchanged in order to achieve this: ion energy per unit atomic mass; ion dose expressed in DPA (displacements per atom), which is the average number of displacements per target atom at the depth corresponding to the maximum elastic energy loss of bombarding ions; and current density expressed in *DPA*/s. With these conditions fulfilled, the only difference between atomic and molecular irradiation should consist in the density of collision cascades. The values of *DPA* were calculated as $DPA = n_v \cdot \Phi / n_{at}$, where $n_v$ is the average total density of vacancies generated by a single ion in both sublattices at the depth corresponding to the maximum elastic energy loss, Φ is the irradiation dose in $cm^{-2}$, and $n_{at} = 1.03 \cdot 10^{23}\,cm^{-3}$ is the atomic density of $\alpha$-$Ga_2O_3$. The TRIM code (version SRIM-2013) [24] was used to calculate *DPA*. The threshold displacement energy was set to $E_d = 25$ eV for Ga and O sublattices. This choice of $E_d$ was motivated by the following considerations: (1) no experimental data on $E_d$ were found in literature; (2) a specific value of the threshold displacement energy has an effect on the number of vacancies obtained in calculations, but does not alter the pattern of distribution of elastic loss with depth within the target; (3) the same value of $E_d = 25$ eV was used in our earlier calculations of *DPA* for $\beta$-$Ga_2O_3$, and this allows one to compare the data obtained for two polytypes. The calculated profiles of distribution of vacancies, which naturally match the distribution of elastic energy loss of decelerating ions, and the density of implanted ions with depth within the target are shown in arbitrary scale in Fig. 3.

All irradiation parameters used in our experiments are listed in the table.

## 3. Experimental results

The virgin samples are epitaxial $\alpha$-$Ga_2O_3$ films grown on the surface of a sapphire substrate. Their high crystalline quality is verified by the results of XRD analysis. Panoramic spectra featured peaks (spaced somewhat apart) corresponding to diffraction reflections from the $\alpha$-$Al_2O_3$ substrate and the $\alpha$-$Ga_2O_3$ film. Small-sized peaks (note that the scale on the vertical axis is logarithmic) indicating the presence of $\varepsilon$-$Ga_2O_3$ inclusions were also found. Figure 1 presents a part of the XRD pattern in the range of 2Θ angles from 82 to 92°. The maximum near 91° in the spectrum of the virgin sample (spectrum *1* in Fig. 1) corresponds to reflection (0 0 12) from the sapphire substrate, the double maximum around 87° is reflection (0 0 12) of the $\alpha$-phase — ICDD PDF2 01-085-0988 $Ga_2O_3$, $R$-3$c$, and the peak around 83.5° is, presumably, reflection (0 0 8) of the $\varepsilon$-phase — ICDD PDF2 01-082-3196 $(Ga_2O_3)_{1,3}$, $P63mc$. The observed doubling of peaks is attributable to the presence of a doublet in the Cu-$K_\alpha$ line. This doublet is resolved in diffraction, which is indicative of a high crystalline quality of the studied sample. Spectra *2* and *3* correspond to the samples irradiated to a dose of 2 *DPA* with P and $PF_4$ ions, respectively. It can be seen that ion bombardment suppresses the $\alpha$-phase peaks; this effect is more pronounced in the case of irradiation with $PF_4$ ions. This provides qualitative evidence of destruction of the crystal structure and faster accumulation of damage under irradiation with molecular ions. The $\varepsilon$-phase peaks vanish completely in both cases. At the same time, no broadening of lines is observed after irradiation; it is thus

Irradiation parameters

| Ion | Energy | | Dose per 1 *DPA* | Flux density | | |
|---|---|---|---|---|---|---|
| | keV | keV/amu | $10^{14}$ cm$^{-2}$ | $10^{11}$ cm$^{-2}\cdot$ s$^{-1}$ | $\mu$A/cm$^2$ | $10^{-3}$ *DPA*/c |
| $P^+$ | 40 | 1.3 | 6.28 | 15.1 | 0.242 | 2.41 |
| $PF_4^+$ | 140 | 1.3 | 1.97 | 4.74 | 0.076 | 2.41 |

fair to assume that the crystal does not accumulate any significant elastic stress.

The discovered difference in formation of structural defects warrants further study. Rutherford backscattering spectra were recorded for this purpose. Figure 2 presents the RBS/C spectra before and after irradiation of $\alpha$-$Ga_2O_3$

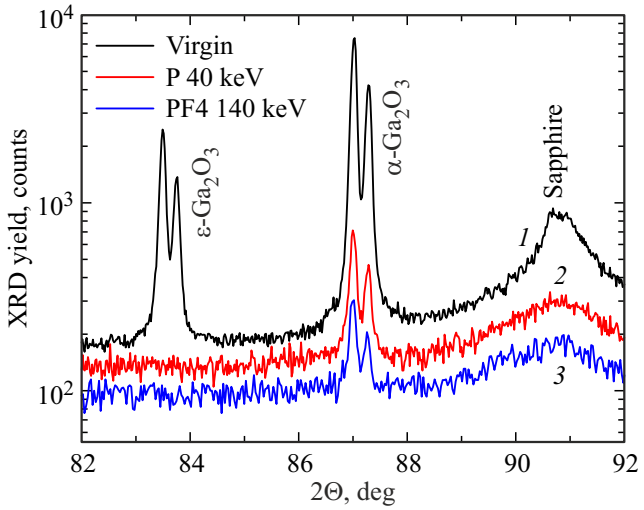


**Figure 1.** XRD spectra of the virgin $\alpha$-$Ga_2O_3$ sample (*1*) and the samples irradiated with 40 keV P ions (*2*) and 140 keV $PF_4$ ions (*3*) to a dose of 2 *DPA*.

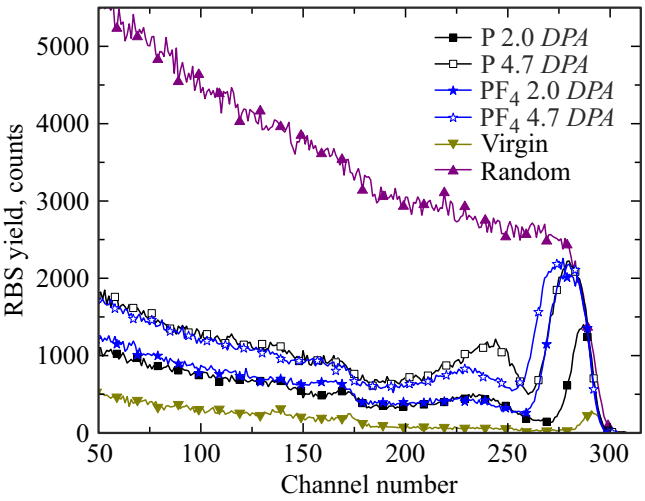


**Figure 2.** RBS/C spectra of $\alpha$-$Ga_2O_3$ samples in random and channeled direction before (*virgin*) and after irradiation with 40 keV P ions (squares) and 140 keV $PF_4$ ions (stars) to a dose of 2.0 *DPA* (filled symbols) and 4.7 *DPA* (open symbols).

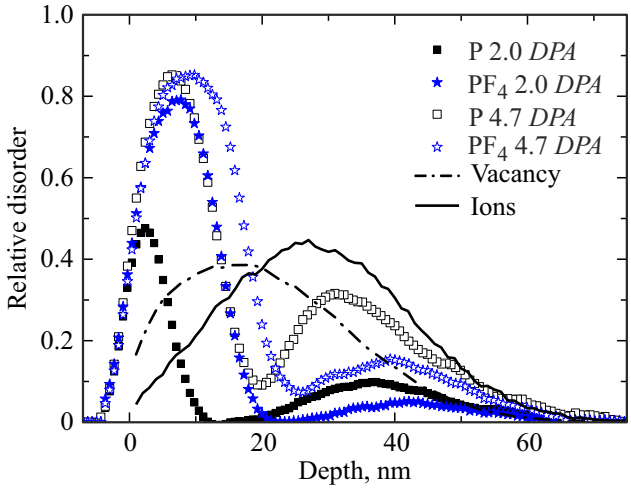


**Figure 3.** Profiles of relative disorder of $\alpha$-$Ga_2O_3$ after irradiation with 40 keV P ions (squares) and 140 keV $PF_4$ ions (stars) to a dose of 2.0 *DPA* (filled symbols) and 4.7 *DPA* (open symbols), distribution of implanted 40 keV P ions (solid curve), and the corresponding profile of elastic energy loss (dash-and-dot curve) in arbitrary scale calculated in TRIM.

with P and $PF_4$ ions. It can be seen that the resulting damage is bimodal for both types of ions. In other words, it has two marked maxima: surface defect maximum (SDM), which corresponds to the near-surface disordered layer, and bulk defect maximum (BDM). The height of both peaks increases with dose, reflecting the accumulation of damage in the target. It is seen clearly that the differences in degree and distribution of damage induced by atomic and molecular ions are very significant. Conspicuous is the fact that the irradiation doses needed to produce detectable damage in the RBS/C spectra for the $\alpha$-phase are appreciably higher than the corresponding doses for the $\beta$-phase (see, e.g., [18,20,25,26]).

All RBS/C spectra were processed using a standard algorithm [27], and depth profiles of relative lattice disorder were plotted. The obtained dependences are shown in Fig. 3 together with the distributions of implanted ions and generated displacements calculated using the TRIM code in the binary collision approximation [22]. The emergence of bimodal distributions of structural damage is seen even more clearly in Fig. 3. Note also that the SDM width for molecular ions is significantly higher than the corresponding width in the case of irradiation with atomic ions to the same dose. The difference becomes less noticeable as the

dose increases to 4.65 *DPA*; apparently, this is attributable to the saturation of growth occurring when the disorder level becomes close to the level of complete amorphization. However, just as in the case of ion implantation into the $\beta$-phase of gallium oxide, complete amorphization is not observed. At the same time, the BDM corresponding to atomic ions is higher at both doses than the peak representing molecular irradiation. In addition, the BDM is positioned significantly deeper than the maximum of elastic ion energy loss. This is another feature that differentiates the results of our experiments from the data published earlier for $\beta$-$Ga_2O_3$ [18,20,25].

## 4. Discussion of results

As was already noted, the energy of an ion penetrating a solid body is transferred to electrons and atoms of the target. The elastic energy loss is the primary channel of such transfer, which induces the formation of crystal structure defects, in semiconductors and metals: ions collide with atoms and displace them from crystal lattice sites [8]. Displaced atoms acquire a certain energy and may, in turn, collide with other atoms, knocking them out of their positions, and so on. A collision cascade of vacancies and interstitial atoms forms as a result. It was already understood in early work [28–30] that volumetric density $f_{av}$ is an important parameter of such cascades. We have developed an algorithm for calculating $f_{av}$ based on the data obtained in TRIM [23,31]. This algorithm was used in the present study to calculate the cascade density and the fraction of ions producing at least one subcascade at a given depth. The obtained results are shown in Fig. 4. It can be seen that the density of an individual cascade formed by a molecular $PF_4$ ion in the near-surface region is higher than the density corresponding to an atomic P ion. This is attributable to the fact that atoms constituting a molecule enter the target as a tight group. Having traveled for several angstroms deeper into the target, a molecule decomposes into constituent atoms, which continue moving independently [32]. Each of them produces its own collision cascade. Since these cascades originate essentially from one and the same point, they overlap near the surface, and the density of the summary molecular cascade increases. At greater depths, the trajectories of atoms originating from a molecular ion diverge, and the cascades cease to overlap. From a certain depth onward, the molecular cascade density is defined solely by the density of individual atomic cascades. Naturally, this depth for fluorine atoms is shallower than the corresponding depth for phosphorus atoms, since the mass of fluorine is lower. These features of development of individual displacement cascades provide an explanation both for the observed broadening of the near-surface disordered layer under irradiation with molecular ions and for the difference in patterns of BDM growth under the same equivalent doses of irradiation with P and $PF_4$ ions. Indeed, the increased density of individual cascades

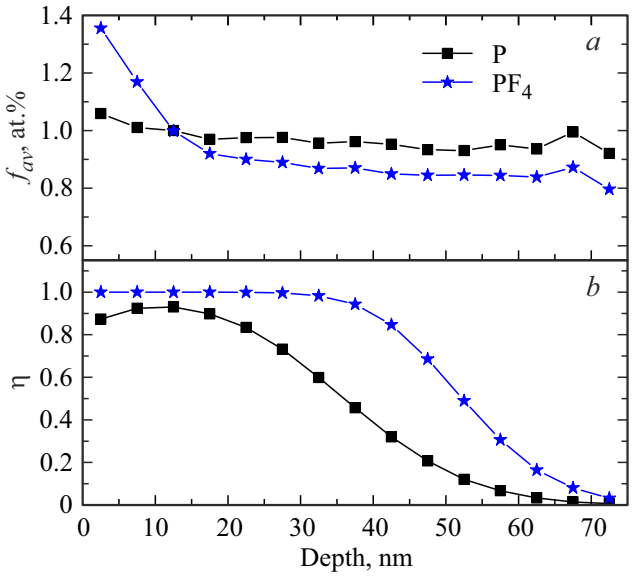


**Figure 4.** *a* — Average density of individual collision cascades $f_{av}$ formed in the target. *b* — Fraction of ions $\eta$ producing at least one subcascade within 5 nm of a given depth. Squares and stars correspond to P and $PF_4$ ions, respectively.

of $PF_4$ ions near the surface translates into faster SDM growth (the mechanism of SDM thickening was discussed, e.g., in [33]). The density of cascades of a molecular $PF_4$ ion in the bulk (outside of the near-surface region) is formed by four F atoms and one P atom and turns out to be lower than the cascade density for an atomic ion. Therefore, the BDM after bombardment of $\alpha$-$Ga_2O_3$ with molecular ions is also smaller (see Fig. 3). As the ion dose increases, the surface disordered layer gets thicker, and its inner boundary shifts deeper into the sample. The region of cascade overlap within an intact crystal becomes ever smaller. Thus, the rates of SDM growth for two type of ions become almost equal, and the relative difference in SDM thickness for them decreases.

It should also be noted that the depth of BDM localization in $\alpha$-$Ga_2O_3$ is close to the position of the maximum of the distribution of implanted ions; this distinguishes $\alpha$-$Ga_2O_3$ from the $\beta$-phase. It bears reminding that the depth of BDM formation for it matches the maximum of ballistic displacements [18,20,25]. The ion doses needed to induce the same level of crystal structure damage also differ appreciably: the dose for $\alpha$-$Ga_2O_3$ is almost an order of magnitude higher than the one for $\beta$-$Ga_2O_3$. These facts indicate that the physical mechanisms of buildup of stable structural damage in different polytypes of gallium oxide are significantly dissimilar.

## 5. Conclusion

The accumulation of radiation damage in $\alpha$-$Ga_2O_3$ under bombardment with atomic $P^+$ and molecular $PF_4^+$ ions was

examined. The observed distributions of stable structural damage have two peaks (surface and bulk defect maxima) in both cases. The ion dose needed to induce a certain level of disorder in metastable $\alpha$-$Ga_2O_3$ is $\sim 10$ times higher than the dose corresponding to roughly the same disorder level in the stable $\beta$-phase. The bulk defect maximum in $\alpha$-$Ga_2O_3$ is positioned deeper than the maximum of elastic ion energy loss and is close to the maximum of the distribution of implanted particles. It was demonstrated that molecular ions induce more damage in the near-surface region, therefore, the thickness of the surface disordered layer grows faster. At the same time, the magnitude of the bulk defect maximum grows slower under irradiation with molecular ions (within the considered dose range) than in experiments with atomic ions. Compared to atomic ions, the density of individual collision cascades of molecular ions is higher near the surface and lower in the bulk of a sample. Thus, the density of collision cascades exerts a significant influence on the processes of radiation-induced defect formation in $\alpha$-$Ga_2O_3$ both in the bulk of a target and near its surface.

### Funding

This study was supported by the Russian Science Foundation, grant No. 22-19-00196.

### Conflict of interest

The authors declare that they have no conflict of interest.

## References

[1] P.J. Wellmann, Z. Anorg. Allg. Chem., **643**, 1312 (2017). Doi: 10.1002/zaac.201700270
[2] S.I. Stepanov, V.I. Nikolaev, V.E. Bougrov, A.E. Romanov. Rev. Adv. Mater. Sci., **44**, 63 (2016).
[3] S.J. Pearton, F. Ren, M. Mastro (eds). *Gallium Oxide. Technology, Devices and Applications* (Elsevier Inc., 2019).
[4] S.J. Pearton, F. Ren, M. Tadjer, J. Kim. J. Appl. Phys., **124**, 220901 (2018). Doi: 10.1063/1.5062841
[5] A. Nikolskaya, E. Okulich, D. Korolev, A. Stepanov, D. Nicolichev, A. Mikhaylov, D. Tetelbaum, A. Almaev, Ch.A. Bolzan, A. Buaczik, jr., R. Giulian, P.L. Grande, A. Kumar, M. Kumar, D. Gogova. J. Vac. Sci. Technol., **39**, 030802 (2021). Doi: 10.1116/6.0000928
[6] E. Ahmadi, Y. Oshima. J. Appl. Phys., **126**, 160901 (2019). Doi: 10.1063/1.5123213
[7] A.Y. Polyakov, V.I. Nikolaev, E.B. Yakimov, F. Ren, S.J. Pearton, J. Kim. J. Vac. Sci. Tech. A, **40**, 020804 (2022). Doi: 10.1116/6.0001701
[8] W. Wesch, E. Wendler. *Ion Beam Modification of Solids: Ion-Solid Interaction and Radiation Damage* (eds) (Springer Cham, 2016). Doi: 10.1007/978-3-319-33561-2
[9] A.I. Titov, A.Yu. Azarov, L.M. Nikulina, S.O. Kucheyev. Phys. Rev. B, **73**, 064111 (2006). Doi: 10.1103/PhysRevB.73.064111
[10] A.I. Titov, S.O. Kucheyev, V.S. Belyakov, A.Yu. Azarov. J. Appl. Phys., **90**, 3867 (2001). Doi: 10.1063/1.1404426
[11] J.B. Wallace, L.B. Bayu Aji, L. Shao, S.O. Kucheyev. Phys. Rev. Lett., **120**, 216101 (2018). Doi: 10.1103/PhysRevLett.120.216101
[12] L.B. Bayu Aji, J.B. Wallace, S.O. Kucheyev. Sci. Rep., **7**, 4703 (2017). Doi: 10.1038/srep44703
[13] A.Yu. Azarov, S.O. Kucheyev, A.I. Titov, P.A. Karaseov. J. Appl. Phys., **102**, 083547 (2007). Doi: 10.1063/1.2801404
[14] A.I. Titov, P.A. Karaseov, V.S. Belyakov, K.V. Karabeshkin, A.V. Arkhipov, S.O. Kucheyev, A. Azarov. Vacuum, **86**, 1638 (2012). Doi: 10.1016/j.vacuum.2011.12.014
[15] P.A. Karaseov, K.V. Karabeshkin, E.E. Mongo, A.I. Titov, M.W. Ullah, A. Kuronen, F. Djurabekova, K. Nordlund. Vacuum, **129**, 166 (2016). Doi: 10.1016/j.vacuum.2016.01.011
[16] A. De Backer, A.E. Sand, K. Nordlund, L. Luneville, D. Simeone, S.L. Dudarev. EuroPhys. Lett., **115**, 26001 (2016). Doi: 10.1209/0295-5075/115/26001
[17] A. Delcorte, P. Bertrand, B.J. Garrison. J. Phys. Chem. B, **105**, 9474 (2001). Doi: 10.1021/jp011099e
[18] K.V. Karabeshkin, A.I. Struchkov, A.I. Titov, A. Azarov, D. Gogova, P. Karaseov. Springer Proceedings in Physics, **268**, 255 (2022). Doi: 10.1007/978-3-030-81119-8_27
[19] A.I. Titov, V.S. Belyakov, S.O. Kucheyev. Nucl. Instr. Meth. Phys. Res. B, **194**, 323 (2002). Doi: 10.1016/S0168-583X(02)00784-X
[20] A.I. Titov, K.V. Karabeshkin, A.I. Struchkov, V.I. Nicolaev, A.E. Azarov, D.S. Gogova, P.A. Karaseov. Vacuum, **200**, 111005 (2022). Doi: 10.1016/j.vacuum.2022.111005
[21] A.I. Pechnikov, S.I. Stepanov, A.V. Chikiryaka, M.P. Sheglov, M.A. Odnobludov, V.I. Nicolaev. Semiconductors, **53**, 780 (2019). Doi: 10.1134/S1063782619060150)
[22] A.Yu. Azarov, A.I. Titov. Semiconductors, **41**, 7 (2007). Doi: 10.1134/S1063782607010022)
[23] P.A. Karaseov, A.Yu. Azarov, A.I. Titov, S.O. Kucheyev. Semiconductors, **43**, 691 (2009). Doi: 10.1134/S1063782609060013)
[24] J.F. Ziegler, J.P. Biersack, U. Littmark. *The Stopping and Range of Ions in Solids* (Pergamon Press, N.Y., 1985). SRIM-2013 software package available at http://www.srim.org Doi: 10.1007/978-1-4615-8103-1_3
[25] E. Wendler, E. Treiber, J. Baldauf, S. Wolf, C. Ronnig. Nucl. Instr. Meth. Phys. Res. B, **379**, 85 (2016). Doi: 10.1016/j.nimb.2016.03.044
[26] S.B. Kjeldby, A. Azarov, P.D. Nguyen, V. Venkatachalapathy, R. Miksova, A. Mackova, A. Kuznetsov, Ø. Prutz, L. Vines. J. Appl. Phys., **131**, 125701 (2022). Doi: 10.1063/5.0083858
[27] K. Schmid. Radiat. Eff., **17**, 201 (1973). Doi: 10.1080/00337577308232616
[28] J.A. Brinkman. J. Appl. Phys., **25**, 961 (1954). Doi: 10.1063/1.1721810
[29] D.A. Thompson. Radiat. Eff., **56**, 105 (1981). Doi: 10.1080/00337578108229885
[30] J.A. Davies. *High Energy Density Collision Cascades and Spike Effects, p.81, in Ion Implantation and Beam Processing*, ed. by J.S. Williams, J.M. Poate (Sydney, Academic Press, 1984). Doi: 10.1016/B978-0-12-756980-2.50008-4

[31] S.O. Kucheyev, A.Yu. Azarov, A.I. Titov, P.A. Karaseov, T.M. Kuchumova. J. Phys. D: Appl. Phys., **42**, 085309 (2009). Doi: 10.1088/0022-3727/42/8/085309
[32] M.W. Ullah, A. Kuronen, K. Nordlund, F. Djurabekova, P.A. Karaseov. J. Appl. Phys., **112**, 043517 (2012). Doi: 10.1063/1.4747917
[33] A.I. Titov, V.S. Belyakov, A.Yu. Azarov. Nucl. Instr. Meth. Phys. Res. B, **212**, 169 (2003). Doi: 10.1016/S0168-583X(03)01486-1